

1 **Lower Silurian stromatolites in shallow-marine environments of**  
2 **the South China Block (Guizhou Province, China) and their**  
3 **palaeoenvironmental significance**

4  
5 Yue Li<sup>a,\*</sup>, Guan Wang<sup>b</sup>, Stephen Kershaw<sup>c</sup>, Shenyang Yu<sup>a,d</sup>, Chao Ni<sup>a,d</sup>

6 <sup>a</sup> Key Laboratory of Economic Stratigraphy and Palaeogeography, Nanjing Institute  
7 of Geology and Palaeontology, Chinese Academy of Sciences, Nanjing 210008, P R  
8 China,

9 <sup>b</sup> South China Sea Institute of Oceanology, Chinese Academy of Sciences,  
10 Guangzhou, 510301, P R China

11 <sup>c</sup> Institute for the Environment, Brunel University, Uxbridge, UB8 3PH, UK

12 <sup>d</sup> University of Chinese Academy of Sciences, Beijing 100049, P R China

13 \* Corresponding author (Yue Li): E-mail address: [yueli@nigpas.ac.cn](mailto:yueli@nigpas.ac.cn)

14

15 **Abstract**

16 In northern Guizhou Province (Upper Yangtze Platform, South China Block) two  
17 types of reef communities developed in the Lower Silurian (upper Aeronian,  
18 Llandovery) Shihniulan Formation; they are calcimicrobial- and metazoan-dominated  
19 structures, and existed because of northward deepening of the shallow-marine ramp  
20 setting in which they grew. Stromatolitic communities are the focus of the present  
21 study and dominated the shallowest reef structures, while metazoan-dominated reefs,  
22 previously described in other papers, grew in the outer shelf portion of the ramp.

23 Stromatolitic reefs occur in several sections (Daijiagou, Baishanxi, Jianba and  
24 Lianghekou), palaeogeographically close to Qianzhong Land. Within the stromatolite  
25 units, laminar sheets of microbial mats and columns are pronounced, with individual  
26 stromatolite thicknesses generally less than one meter. Some very small stromatolites  
27 are only centimeters in diameter and thickness. Stromatolitic units are cyanobacterial  
28 bindstones mostly associated with shales, siltstones and thin-bedded bioclastic  
29 limestones. Their growth was frequently punctuated by siliciclastic sediments, and  
30 their shallow-water nature is demonstrated by association with birds-eye structures,  
31 cross-stratified sediments, and *Lingulella*-bearing silts in intertidal or/and lagoonal  
32 environments. The stromatolites formed during a regression and erosion surfaces are  
33 common at the top of the Shihniulan Formation. The Tongzi Uplift, a short-duration  
34 expansion of Qianzhong Land, ended the deposition of the late Aeronian limestones.

35

36 **Keywords:** stromatolite, shallow marine, Shihniulan Formation, Lower Silurian,  
37 north Guizhou, South China Block

38

### 39 **1. Introduction**

40 Following the Hirnantian Stage (latest Ordovician) icehouse climate and global  
41 eustatic sea level fall events (Brenchley, 1984), gradual recovery and reorganization  
42 of epibenthic shelly communities led to the first appearance of coral-stromatoporoid  
43 patch reefs in the Rhuddanian Hilliste Formation of the Baltic Basin (Nestor, 1997).

44 The Aeronian Epoch (Middle Llandovery, Silurian) was a time of global recovery of

45 reef-building communities (e.g. Li and Kershaw, 2003; Copper and Jin, 2012), most  
46 likely due to the warmth of marine waters at that time (Li et al., 2008). An 80  
47 million-year period of greenhouse conditions began in the Llandovery Epoch (Early  
48 Silurian) and lasted until the latest Devonian, thus was optimum for stable  
49 development of reefs (Copper, 1988, 2002). The principal Silurian hermatypic fauna  
50 includes tabulate and rugose corals, stromatoporoids and bryozoans with microbial  
51 structures acting as binders in most cases (e.g. Scrutton, 1988; Copper and Brunton,  
52 1991; Brunton and Copper, 1994; Brunton et al., 1998; Copper, 2002; Nose, 2006).  
53 Nevertheless, typical Silurian stromatolites formed of purely cyanobacterial  
54 bindstones are not common; they are quite limited in time and space and less  
55 documented (Brett, 1991; Cao, 1996; Soja and Antoshkina, 1997).

56 Silurian limestones and reefs in the South China Block occur in only the  
57 Llandovery sequences temporally and geographically in what is termed the Upper  
58 Yangtze Platform (western part of the South China Block; e.g. Zhang et al., 1994;  
59 Wan et al., 1997). Late Aeronian reef types in north Guizhou are mainly metazoan  
60 framework-dominated structures in an outer-shelf setting (Wang et al., 2014). Coeval  
61 stromatolitic units at the Daijiagou section, Tongzi County, were first recognized by  
62 the senior author of this paper in the winter of 2005, and also previously recorded in  
63 lithological logging by Zhan and Jin (2007). That unit and three more  
64 stromatolite-bearing sections are investigated here and altogether the stromatolites  
65 occupy a narrow belt spatially. Accordingly, this paper aims to place these unusual  
66 stromatolitic units in perspective of Silurian reef studies. We describe the

67 morphological and lithological features of the stromatolites and discuss their  
68 depositional setting during a regressional process. This study therefore provides better  
69 understanding of the palaeogeographical implications of these Silurian stromatolites  
70 following the end-Ordovician biotic crisis.

71 Facies described in this paper were studied by field observations and logging,  
72 followed by hand specimen and thin section study to characterize the material.  
73 Comparisons with literature facilitated the discussion.

74

## 75 **2. Geological setting**

76 Coeval to the reef-bearing units in Anticosti, Laurentia and Baltica, those in the  
77 South China Block were also situated within the low latitudes of the southern  
78 hemisphere in Early Silurian time (Scotese et al., 1985; McKerrow and Scotese, 1990;  
79 Golonka, 2002). Northern Guizhou lay in the southwestern part of the Yangtze  
80 Platform in an epicontinental sea during Silurian time. Qianzhong Land, in the  
81 southern part of the study area, played a primary role in configuration of biofacies and  
82 lithofacies differentiations of the area (e.g. Rong et al., 2003), leading to  
83 interpretations of water depth. The near-shoal belt close to Qianzhong Land in  
84 northeastern Guizhou was a shallow, well-oxygenated environment in Rhuddanian  
85 time (earliest Silurian). Carbonate facies with shelly benthic communities were  
86 gradually reconstructed after the reef-building gap of the Hirnantian Stage cold  
87 interval (Ni et al., 2015). The first reefs to appear after the extinction are small-scale  
88 coral-stromatoporoid patch reefs in the middle Aeronian upper Xiangshuyuan

89 Formation in Shiqian area, northeastern Guizhou Province (Li and Kershaw, 2003).  
90 Coeval graptolitic black shales of anoxic marine-floor had a much wider distribution  
91 regionally including north Guizhou, so reefs were able to form in only limited areas.  
92 Updated litho- and biostratigraphic correlation schemes suggest that Llandovery  
93 sequences in north Guizhou are comprised of shales and siltstones of the Lungmachi  
94 Formation (mainly of Rhuddanian-Middle Aeronian), limestone-dominated  
95 Shihniulan Formation (late Aeronian) and siltstones-sandstones of the Hanchiatien  
96 Formation (lower Telychian) in ascending order. They were all deposited in a ramp  
97 setting deepening seaward to the north (e.g. Chen et al., 2001; Zhan and Jin, 2007).  
98 Terrigenous-dominated depositional units of the Lungmachi Formation ended in late  
99 Aeronian time. Sequences from Lungmachi to Shihniulan Formations are essentially  
100 regressive. Shallow-marine carbonate facies of the late Aeronian expanded on the  
101 upper Yangtze Platform. The upper Aeronian Shihniulan Formation is ~100 m thick  
102 and is subdivided in ascending order into nodular limestone intercalated with shales  
103 and siltstones of the Songkan Member, and bioclastic and intraclastic bank- and  
104 reef-dominated facies of the Shihniulan Member (Rong et al., 2003).

105 Non-reef lithofacies as well as Llandovery reefs on the Yangtze Platform are  
106 evidence that tectonic uplift and clarity of marine water (low turbidity) were key  
107 factors controlling reef distribution. Ideal conditions in the late Aeronian Epoch  
108 promoted thriving benthic biotas and the formation of diverse bank and reefal units  
109 (Li and Kershaw, 2003; Li and Rong, 2007). The short-duration Tongzi Uplift caused  
110 northward (regressive) migration of the coastline for tens kilometers and terminated

111 carbonate deposition in latest Aeronian time. Sedimentary features such as palaeokarst  
112 surfaces, desiccation mudcracks and birds-eye structures at the top of the Shihniulan  
113 Formation indicate subaerial exposure especially in those near-shoal belt sections of  
114 the Qianzhong Land (Rong et al., 2012; Deng et al., 2012). A transgressional tract of  
115 the early Telychian Hanchiatien Formation in northern Guizhou is mainly composed  
116 of terrigenous debris. Silurian marine facies above the Llandovery are quite rare in the  
117 South China Block due to large-scale tectonic uplift in the Yangtze region (Chen et al.,  
118 1996; Rong et al., 2003).

119 Typical metazoan patch reefs in the Shihniulan Member in the Shuibatang section  
120 of Tongzi County, north Guizhou, which was situated in an outer-shelf belt of the  
121 Yangtze epicontinental sea, were described in preliminary work by Wang et al. (2014).  
122 Equivalent stromatolitic units have limited spatial distributions in north Guizhou and  
123 are confined to the Lianghekou area of Xishui County, the Daijiagou and Baishanxi  
124 areas of Tongzi County, and the Jianba area of Suiyang County. Palaeogeographically  
125 these sections lay along the near-shoal belt near Qianzhong Land (Fig. 1).

126

### 127 **3. Nature of stromatolites**

128 Stromatolites within the Shihniulan Member occur in four sections where the  
129 stromatolite-bearing units terminated at erosion surfaces in all sites due to subaerial  
130 exposure during the Tongzi Uplift (Fig. 2). The overlying strata belong to the  
131 Hanchiatien Formation. Biotic and sedimentary features of the stromatolites, from  
132 west to east, are described next.

133

134 *3.1. Lianghekou section*

135 The stromatolite-bearing unit in the upper Shihniulan Member crops out in a  
136 vertical cliff section at Lianghekou section (GPS 28°7'52.56"N, 106°12'24.60"E).  
137 Here, the Shihniulan Formation sequences below the stromatolites are covered by a  
138 road (Fig. 3A). Column- and mat-shaped stromatolitic units herein are rather thin,  
139 only several centimeters thick individually (Fig. 3B). Below and above the  
140 stromatolites are dark grey calcareous siltstones and shales. Microfacies of the  
141 stromatolites show that dark laminations dominated their structure (Fig. 3C). Some  
142 very small stromatolites are only centimeters in width (Fig. 3D). Light-grey micritic  
143 limestones capping the stromatolites contain birds-eye structures and in some cases  
144 also show stromatolitic texture. Macrofossils are also very rare in these micritic  
145 limestone layers (Fig. 3E). A palaeokarst surface of the Tongzi Uplift occurs at the  
146 top of the Shihniulan Formation (Fig. 3F).

147

148 *3.2. Daijiagou section*

149 Daijiagou section (GPS 28°4'57.04"N, 106°47'0.80"E) is one of the best-known  
150 sites that record complete successions through the Upper Ordovician to Llandovery  
151 sequences in the northern Guizhou areas. Stromatolitic units preliminary reported by  
152 Zhan and Jin (2007) are mainly preserved in Beds 25-26 of the logged section as  
153 described below:

154 Bed 26 (5.7 m thick) comprises dark grey, medium- to thick-bedded argillaceous

155 and bioclastic limestones with some stromatolites occurring in the middle part.

156 Associated bioclastic material is composed of mainly brachiopod fragments, in  
157 samples AFN113-115, but no complete fossils have been found.

158 Bed 25, 13.8 m thick, is dominated by dark grey, thin-bedded argillaceous  
159 limestone with a few intercalations of calcareous mudstone, siltstone, and coral shell  
160 layers. Of 157 AFN106-112 sampled here, Sample AFN107 is a coral shell bed, and  
161 AFN109 stromatolite unit.

162 Of the two major stromatolitic horizons in Beds 25 and 26, the stromatolitic unit  
163 of Bed 25 is about 2 m thick, and formed as an accumulation of low-relief mats (Fig.  
164 4A) with horizontal to curving stromatolitic laminae (Fig. 5A). The stromatolite  
165 morphology, overall, is similar to that in the Late Archean Campbellrand-Malmani  
166 platform of South Africa (Riding, 2011). Bed 26 stromatolites vary from maximum of  
167 1.5 m to about 0.5 m in thickness. They typically formed column-shapes and  
168 cabbage-like morphologies (Fig. 4B-C). Microfacies of laminations show great  
169 similarity to that of algal-mats from Bed 25 except obvious dome-like structures (Fig.  
170 5B).

171 Some small stromatolitic units with thicknesses about 10 cm are uncommonly  
172 found in greyish black shales and siltstones between these two major stromatolitic  
173 units in Bed 25-26. Macrofossils are rare, and represented by few *Eospirifer* and  
174 *Linguella* (Fig. 4D).

175 Siltstones and shales intercalated with some limestone with little macrofossil  
176 content occur above the stromatolite of Bed 26, in which thin-bedded limestone



177 contains cross bedding (Fig. 4, E). A palaeokarst surface is pronounced at the top of  
178 the thin-bedded limestone, indicating an unconformable boundary between the  
179 Shihniulan Formation and the overlying lower Telychian Hanchiatien Formation (Fig.  
180 4F).

181

### 182 *3.3. Baishanxi section*

183 Two stromatolitic units intercalated with thin-bedded bioclastic limestone occur  
184 in the Baishanxi section (GPS: 28°8'4.97"N, 106°56'2.11"E) (Fig. 6A). Therein  
185 columnar stromatolites are pronounced, and they are 0.5 m and 0.7 m thick in the  
186 lower and upper units, respectively (Fig. 6B-C). Most columns are 5-8 cm in diameter.  
187 Individual thicknesses of the laminae are somewhat variable in both lower (Fig. 6D)  
188 and upper (Fig. 6E) stromatolitic units, in which they are largely light-coloured  
189 horizontal laminae.

190

### 191 *3.4. Jianba section*

192 The stromatolitic unit about 1-1.5 m below the top of the Shihniulan Member is  
193 about 0.7 m in thickness at this section (GPS 28°4'20.90"N, 106°2'42.64"E). The base  
194 and top layers of the stromatolitic unit are thin-bedded yellow calcareous siltstones  
195 containing uncommon fine-grained bioclastic components (Fig. 7A). Stromatolites are  
196 column-shaped with individual columns being 3-10 cm in diameter and with the  
197 widest column being 25 cm in diameter (Fig. 7B). Dark laminae are most common  
198 and regularly intercalated with bright laminae. Some horizontal laminae are not very

199 clear due to dolomitization. Fine-grained dolomite is commonly present.

200

## 201 **4. Discussion**

### 202 *4.1. General setting*

203 Most stromatolites described in this paper are underlain or overlain by dark  
204 siltstones and/or shales. Thus sporadic turbidity and possible anoxic lagoonal  
205 conditions are interpreted to have punctuated growth of the microbial communities  
206 and constrained development of the stromatolites. The low diversity and abundance of  
207 brachiopod fauna of *Lingulella* and *Eospirifer* at the Daijiagou section are possibly  
208 indicators of BA1, a benthic association in the very shallow belt close to the land  
209 (based on the well-known benthic assemblage depth scheme described by Ziegler,  
210 1965; Boucot and Johnson, 1973; and Johnson et al., 1985). Cross-stratification in the  
211 Daijiagou sequence also suggests an intertidal to shallow subtidal setting. Micritic  
212 limestones with birds-eye structures above the stromatolites in the Lianghekou section  
213 are similar to the descriptions and environmental interpretations by Ham (1952) and  
214 Flügel (2004); they are indicators of very shallow lime-mud flats occasionally  
215 exposed above sea level. Therefore, the palaeoenvironment is interpreted as lagoonal to  
216 intertidal close to the coastline of the Qianzhong Land and was unfavorable for  
217 diverse metazoan fauna but advantageous for opportunistic taxa of cyanobacteria.

218

### 219 *4.2. Controls on formation of stromatolites*

220 Coral-stromatoporoid reef communities of the Yangtze Platform, South China

221 Block, originated in the Late Ordovician Period; they were strongly affected by the  
222 cooling Hirnantian Stage regression (e.g. Li et al., 2004). Metazoan reef recovery  
223 started in the near-shoal belt of Qianzhong Land in the middle Aeronian  
224 Xiangshuyuan Formation, and can be recognized in the Xiangshuyuan and Baisha  
225 sections, Shiqian, northeastern Guizhou. Carbonate platforms and the  
226 metazoan-dominated biota expanded stepwise towards outer-shelf positions in the late  
227 Aeronian Epoch (Li and Kershaw, 2003); the Shihniulan Formation succession  
228 indicates a full recovery of colonial rugose and tabulate corals, stromatoporoids and  
229 high diversity reef-attached biota. Wang et al. (2014) suggested that these changes  
230 represent a global evolutionary step in the aftermath of the latest Ordovician mass  
231 extinction event, further indicated by coeval global analogues comprising similar  
232 biotic structures in Anticosti (Copper and Jin, 2012) and in Kazakhstan (Berg et al.,  
233 1980; Zadoroshnaya and Nikitin, 1990). About eight major units of carbonate  
234 platforms with a total of 30 patch reefs of the late Telychian Ningqiang Formation  
235 demonstrate the peak stage of Silurian reefs in the northwest margin of the Yangtze  
236 Platform (Li et al., 2002). Therefore, the late Aeronian Epoch is a time of  
237 evolutionary significance for full recovery of reefs. Wide resurgence of  
238 post-extinction microbial buildups of the earliest Silurian in Nevada and Utah  
239 (Sheehan and Harris, 2000, 2004) and the Early Triassic (Schubert and Bottjer, 1992;  
240 Yang et al., 2011; Kershaw et al., 2007, 2012; Chen et al., 2014; Luo et al., 2016)  
241 have been interpreted as anachronistic facies, indicating the harsh environments  
242 following major biotic crises (Sepkoski et al., 1991; Schubert and Bottjer, 1992; Chen

243 and Benton, 2012). However, late Aeronian stromatolitic units documented here were  
244 not evolutionary analogues of a disaster episode. Instead, they are clearly placed as  
245 communities in near-shoal positions co-existing with thriving reefal metazoans that  
246 were present in the outer shelf.

247 Biotic structure and size of reefs are governed by multiple oceanographic  
248 parameters (Copper, 1994a, b) resulting in low biodiversities and simple fabrics in  
249 some Silurian reefs (Watkins, 1979). Silurian stromatolites occurred more frequently  
250 in restricted environments, especially in deep water habitats or hypersaline zones in  
251 which the predating pressure was not as high as that in a typical open reef-setting  
252 (Brett, 1991; Copper and Brunton, 1991). Although the Shihniulan stromatolites grew  
253 in shallow niches, they inhabited similar environmental settings to Silurian  
254 stromatolites of other areas mentioned above. When compared with the worldwide  
255 spread of metazoan-dominated reefs during the Silurian, cyanobacterial buildups  
256 including stromatolites are limited and occurred locally during that time (Textoris and  
257 Carozzi, 1966; Cherns, 1982; Soja and Riding, 1993; Soja, 1994; Soja et al., 2000).  
258 Soja and Antoshkina (1997) inferred ecological similarity and palaeogeographical  
259 significance of Upper Silurian subtidal stromatolites in Alaska and the Ural  
260 Mountains, built by an unusual consortium of microbial taxa in association with  
261 distinctive sphinctozoan sponges. Microbialites and algal framework fabrics are also  
262 present in the Middle-Late Silurian stromatoporoid-tabulate coral reefs in Baltic  
263 Gotland (Nose et al., 2006). In addition to the aspects of biotic evolution, reefs are  
264 also constrained by water depth and turbidity (Li and Kershaw, 2003). The

265 Llandovery sea-level change curves reconstructed worldwide indicate a highstand  
266 level (or transgressional interval) during the late Aeronian (Leggett et al., 1981;  
267 Johnson et al., 1991; Ross and Ross, 1996; Jeppsson et al., 1997; Loydell, 1998; Haq  
268 and Schutter, 2008; Johnson, 2010). Surprisingly, the Shihniulan stromatolites  
269 described in this paper are confined to the intertidal or lagoonal belt close to  
270 Qianzhong Land during the late Aeronian Epoch. The record of the high-frequency  
271 sea-level changes in the near-shoal belt might reflect small-scale sea-level drops in  
272 morphological differentiations of algal-mats and column-shape stromatolites. The  
273 sedimentary features, especially in subaerially exposed surfaces at the top of the  
274 Shihniulan Formation from the near-shoal facies sections mentioned above, reinforce  
275 our view that the Tongzi Uplift played a key role in configuration of the distribution  
276 of land and sea regionally. Sporadic inputs of muddy and silty debris in near-shoal  
277 belts also affected the growth of the stromatolites in the northern Guizhou areas. Such  
278 a turbid environmental setting is attributed to gradual expansion of land during the  
279 Tongzi Uplift (Rong et al., 2012).

280

## 281 **5. Conclusions**

282 A wide carbonate ramp with northward-deepening sea was favorable for  
283 differentiation of reef communities in the upper Aeronian (Llandovery, Silurian)  
284 Shihniulan Formation in northern Guizhou. Distinctive stromatolites formed solely by  
285 cyanobacterial communities are restricted to the near-shoal belt close to Qianzhong  
286 Land; coeval metazoan reefs occupied the outer shelf. Deposition of siliciclastic

287 sediment in this marginal marine environment constrained the size of the stromatolites.  
288 Termination of the Shihniulan Formation as well as calcimicrobial inhabitation was  
289 mainly caused by shallowing up, including subaerial exposure, due to the northern  
290 seaward migration of the coastline during the Tongzi Uplift episode. Overall, the  
291 Shihniulan stromatolites are interpreted as one of a subfacies of a reef complex  
292 together with metazoan reefs from the outer shelf.

293

294 **Acknowledgements:** We are grateful to anonymous referees for their valuable  
295 comments on our manuscript. Thanks are also due to Prof. Jiayu Rong in NIGPAS for  
296 guilding in the field excursion. We offer our sincere gratitude to Prof. Thomas Algeo  
297 and Prof. Zhongqiang Chen for editing. This study was supported by National Natural  
298 Science Foundation of China (granted No. 41072002, 41372022, XDB10010503 and  
299 41521061).

300

## 301 **References**

- 302 Berg, L.S., Keller, B.M., Kovalevskii, O.P., Tolmacheva, S.G., Palets, L.M.,  
303 Bandaletov, S.M., Olenicheva, M.A., 1980. Chu-Iliiskii rudnyi polyas,  
304 Geologiya Chu-iliiskovo raiona [Chu-Ili Mining Camp Geology of the Chu-Ili  
305 Region]. Nauka, Alma-Ata 1–503 (in Russian).
- 306 Boucot, A.J., Johnson, J.G., 1973. Silurian brachiopods. In: Hallam, A., (ed.), Atlas of  
307 Palaeobiogeography, Elsevier, Amsterdam, 59–65.
- 308 Brenchley, P.J., 1984. Late Ordovician Extinctions and their relationship to the

309 Gondwana Glaciation. In: Brenchley, P.J. (Ed.), *Fossils and Climate*. John  
310 Wiley and Sons, Inc. pp. 291–327.

311 Brett, C.E., 1991. Organism-sediment relationships in Silurian marine environments.  
312 In: Bassett, M.G., Lane, P.D., Edward, D. (Eds.), *The Murchison Symposium:*  
313 *Proceedings of an International Conference on the Silurian System*. Spec. Pap.  
314 *Palaeontol.* 44, pp. 301–344.

315 Brunton, F.R., Copper, P., 1994. Paleocology, temporal, and spatial analysis of Early  
316 Silurian reefs of the Chicotte Formation, Anticosti Island, Quebec, Canada.  
317 *Facies* 31, 57–80.

318 Brunton, F.R., Smith, L., Dixon, O.A., Copper, P., Kershaw, S., Nestor, H., 1998.  
319 Silurian reef episodes, changing seascapes, and paleobiogeography. New York  
320 State Mus. Bull. 491, 265–282.

321 Cao, R.G., 1996. Cambrian and Silurian stromatolites in eastern Yunnan. *Reg. Geol.*  
322 *Chin.* 27–30. (in Chinese)

323 Chen, X., Rong, J.Y., Wang, C.Y., Geng, L.Y., Deng, Z.Q., Wu, H.J., Chen, T.E., Xu,  
324 J.T., Holland, C.H., Aldridge, R.J., Bassett, M.G., Downie, C., Lane, P.D.,  
325 Richards, R.B., Scrutton, C.T., 1996. Telychian (Llandovery) of the Yangtze  
326 region and its correlation with British Isles. Beijing (Science Press), 162pp (in  
327 Chinese with English summary).

328 Chen, X., Rong, J.Y., Zhou, Z.Y., Zhang, T.D., Zhan, R.B. Liu, J.B., Fan, J.X., 2001.  
329 The central Guizhou and Yichang uplifts, Upper Yangtze region, between  
330 Ordovician and Silurian. *Chin. Sci. Bull.* 46, 1580–1584.

331 Chen, Z.Q., Benton, M.J., 2012. The timing and pattern of biotic recovery following  
332 the end-Permian mass extinction. *Nat. Geosci.* 5, 375–383.

333 Chen, Z.Q., Wang, Y.B., Kershaw, S., Luo, M., Yang, H., Zhao, L.S., Fang, Y.H.,  
334 Chen, J.B., Li, Y., Zhang, L., 2014. Early Triassic stromatolites in a siliciclastic  
335 nearshore setting in northern Perth Basin, Western Australia: geobiologic  
336 features and implications for post-extinction microbial proliferation. *Glob.*  
337 *Planet. Chang.* 121, 89–100.

338 Cherns, L., 1982. Palaeokarst, tidal erosion surfaces and stromatolites in the Silurian  
339 Eke Formation of Gotland, Sweden. *Sedimentology* 29, 819–833.

340 Copper, P., 1988. Ecological succession in Phanerozoic reef ecosystems: is it real?.  
341 *Palaios* 3, 136–151.

342 Copper, P., 1994a. Reef under stress: the fossil record. *Cour. Forschungsinst.*  
343 *Senckenberg* 172, 87–94.

344 Copper, P., 1994b. Ancient reef ecosystem expansion and collapse. *Coral reefs* 13, 3–  
345 11.

346 Copper, P., 2002. Silurian and Devonian reefs: 80 million years of global greenhouse  
347 between two ice ages. In: Kiessling, W., Flügel, E., Golonka, J. (Eds.),  
348 *Phanerozoic Reef Patterns*. SEPM Special Publication 72, pp. 181–238.

349 Copper, P., Brunton, F., 1991. A global review of Silurian reefs. In: Bassett, M.G.,  
350 Lane, P.D., Edward, D. (Eds.), *The Murchison Symposium: Proceedings of an*  
351 *International Conference on the Silurian System*. *Spec. Pap. Palaeontol.* 44, pp.  
352 225–260.



353 Copper, P., Jin, J.S., 2012. Early Silurian (Aeronian) East Point coral patch reefs of  
354 Anticosti Island, Eastern Canada: first reef recovery from the  
355 Ordovician/Silurian Mass Extinction in Eastern Laurentia. *Geosciences* 2, 64–  
356 89.

357 Deng, X.J., Wang, G., Li, Y., 2012. Sedimentary characteristics at the top of the  
358 Shihniulan Formation (late Aeronian, Silurian) and their implications for  
359 identification of the shoal line in Tongzi, Northern Guizhou. *J. Stratigr.* 36,  
360 718–722 (in Chinese with English summary).

361 Flügel, E., 2004. *Microfacies of carbonate rocks: analysis, interpretation and*  
362 *application*. Heidelberg: Springer–Verlag, 1–984.

363 Golonka, J., 2002. Plate tectonic maps of the Phanerozoic. In: Kiessling, W., Flügel,  
364 E., Golonka, J. (Eds.), *Phanerozoic Reef Patterns*. SEPM Special Publication 72,  
365 pp. 21–75.

366 Ham, W.E., 1952. Algal origin of the "Birdseye" limestone in the McLish Formation.  
367 *Proc. Oklahoma Acad. Sci.* 33, 200–203.

368 Haq, B.U., Schutter, S.R., 2008. A chronology of Paleozoic sea-level changes.  
369 *Science* 322, 64–68.

370 Jeppsson, L., 1997. Recognition of a probable secundo-primario event in the Early  
371 Silurian. *Lethaia* 29, 311–315.

372 Johnson, M.E., 2010. Tracking Silurian eustasy: alignment of empirical evidence or  
373 pursuit of deductive reasoning?. *Palaeogeogr. Palaeoclimatol. Palaeoecol.* 296,  
374 276–284.

375 Johnson, M.E., Rong, J.Y., Yang, X.C., 1985. International correlation by sea-level  
376 events in the Early Silurian of North America and China. *Bull. Geol. Soc.*  
377 London, 81, 343-385.

378 Johnson, M.E., Kaljo, D., Rong, J.Y., 1991. Silurian eustasy. In: Bassett M.G.,  
379 Edwards, D. (Eds.), *The Murchison Symposium – Proceedings of an*  
380 *International Conference on the Silurian System. Spec. Pap. Palaeontol.* 44, pp.  
381 145–163.

382 Kershaw, S., Li, Y., Crasquin-Soleau, S., Feng, Q.L., Mu, X.N., Collin, P.Y.,  
383 Reynolds, A., Guo, L., 2007. Earliest Triassic microbialites in the South China  
384 block and other areas: controls on their growth and distribution. *Facies* 53, 409–  
385 425.

386 Kershaw, S., Crasquin, S., Li, Y., Collin, P.Y., Forel, M.B., Mu, X.N., Baud, A.,  
387 Wang, Y., Xie, S.C., Maurer, F., Gou, L., 2012. Microbialites and global  
388 environmental change across the Permian–Triassic boundary: a synthesis.  
389 *Geobiology* 10, 25–47.

390 Leggett, J.K., McKerrow, W.S., Cocks, L.R.M., Richards, R.B., 1981. Periodicity in  
391 the early Palaeozoic marine realm. *J. Geol. Soc. Lon.* 138, 167–176.

392 Li, Y., Kershaw, S., Chen, X., 2002. Biotic structure and morphology of patch reefs  
393 from South China (Ningqiang Formation, Telychian, Llandovery, Silurian).  
394 *Facies* 46, 133–148.

395 Li, Y., Kershaw, S., 2003. Reef reconstruction after extinction event of Latest  
396 Ordovician in Yangtze Platform, South China. *Facies* 48, 269–284.

- 397 Li, Y., Kershaw, S., Chen, X., 2004. Control of carbonate sedimentation and reef  
398 growth in Llandovery sequences on the northwestern margin of Yangtze  
399 Platform, South China. *Gondwana Res.* 7 (4), 937–949.
- 400 Li, Y., Rong, J.Y., 2007. Shell concentrations of Early Silurian virgianid brachiopods  
401 in northern Guizhou: Temporal and spatial distribution and tempestite  
402 formation. *Chin. Sci. Bull.* 52, 1680–1691.
- 403 Li, Y., Wang, J.P., Zhang, Y.Y., Gu, C.G., 2008. Perspective of carbonates during the  
404 Ordovician-Silurian transition in South China: implications of their  
405 palaeoclimate response. *Progr. Nat. Sci.* 18(10): 122–128. (in Chinese)
- 406 Loydell, D.K., 1998. Early Silurian sea-level changes. *Geol. Mag.* 135, 447–471.
- 407 Luo, M., Chen, Z.Q., Shi, G.R., Fang, Y.H., Song, H.J., Jia, Z.H., Huang, Y.G., Yang,  
408 H., 2016. Upper Lower Triassic stromatolite from Anhui, South China:  
409 geobiologic features and paleoenvironmental implications. *Palaeogeogr.*  
410 *Palaeoclimatol. Palaeoecol.* 452, 40–54.
- 411 McKerrow, W.S., Scotese, C.R., 1990. Revised world basemaps. In: McKerrow, W.S.,  
412 Scotese, C.R. (Eds.), *Palaeozoic palaeogeography and biogeography*. Mem.  
413 *Geol. Soc. London.* 12, pp. 1–20.
- 414 Nestor, V., 1997. Reflection of Wenlock oceanic episodes and events on the  
415 chitinozoan succession of Estonia. *Proc. Est. Acad. Sci., Geol.* 46 (3), 119–126.
- 416 Ni, C., Deng, X.J., Li, Y., 2015. Biodiversity of the “Lungmachi Formation”  
417 limestones at the Xiangshuyuan section, Shiqian, NE Guizhou. *Acta*  
418 *Micropalaeontol. Sin.* 32 (1), 96–104 (in Chinese with English summary)

419 Nose, M., Schmid, D.U., Leinfelder, R.R., 2006. Significance of microbialites,  
420 calcimicrobes, and calcareous algae in reefal framework formation from the  
421 Silurian of Gotland, Sweden. *Sediment. Geol.* 192 (3), 243–265.

422 Riding, R., 2011. The nature of stromatolites: 3,500 Million years of history and a  
423 century of research. In: Reitner, J., (eds.), *Advance in Stromatolite Giobiology*.  
424 *Lect. Note Earth Sci.* 131, 29–74.

425 Rong, J.Y., Chen, X., Su, Y.Z., Ni, Y.N., Zhan, R.B., Chen, T.E., Fu, L.P., Li, R.Y.,  
426 Fan, J.X., 2003. Silurian paleogeography of China. In: Landing, E., Johnson,  
427 M.E. (Eds.), *Silurian Lands and Seas-Paleogeography Outside of Laurentia*.  
428 *New York State Mus. Bull.* 493, pp. 243–298.

429 Rong, J.Y., Wang, Y., Zhan, R.B., Huang, B., Wu, R.C., Wang G, Li, Y., Deng, X.J.,  
430 2012. On the Tongzi Uplift: Evidences of northward expansion of Qianzhong  
431 Oldland during Aeronian, Llandovery, Silurian. *J. Stratigr.* 36, 679–691 (in  
432 Chinese with English summary)

433 Ross, C.A., Ross, R.P., 1996. Silurian sea-level fluctuations. In: Witzke, B.J.,  
434 Ludvigson, G.A., Day, J. (Eds.), *Paleozoic Sequence stratigraphy: view from*  
435 *the North American Craton. Geol. Soc. Am. Spec. Pap.* 306, pp. 187–192.

436 Schubert, J.K., Bottjer, D.J., 1992. Early Triassic stromatolites as post-mass  
437 extinction disaster forms. *Geology* 20, 883–886.

438 Schubert, J.K., Bottjer, D.J., 1995. Aftermath of the Permian-Triassic mass extinction  
439 event: Paleoecology of Lower Triassic carbonates in the western USA.  
440 *Palaeogeogr. Palaeoclimatol. Palaeoecol.* 116, 1–39.

441 Scotese, C.R., Van der Voo, R., Barrett, S.F., Westoll, T.S., Chaloner, W.G., 1985.  
442 Silurian and Devonian Base Maps [and Discussion]. *Philos. Trans. R. Soc.*  
443 London, B: *Biol. Sci.* 309 (1138), 57–77.

444 Scrutton, C.T., 1988. Patterns of extinction and survival in Palaeozoic corals. In:  
445 Larwood, G.P. (Ed.), *Extinction and survival in the fossil record*. Clarendon  
446 Press, Oxford, pp. 65–88.

447 Sepkoski, J.J.Jr., Bambach, R.K., Droser, M.L., 1991. Secular changes in Phanerozoic  
448 event bedding and biological overprint. In: Einsele, G., Ricken, W., Seilacher,  
449 A., (Eds.), *Cycles and events in stratigraphy*. Heidelberg: Springer Verlag, 298–  
450 312.

451 Sheehan, P.M., Harris, M.T., 2000. Early Silurian stromatolites and thrombolites:  
452 successful disaster forms after the Late Ordovician mass extinction. *Abstr.*  
453 *Progra. Geol. Soc. Am. Nat. Meeting* 32, 367–368.

454 Sheehan, P.M., Harris, M.T., 2004. Microbialite resurgence after the Late Ordovician  
455 extinction. *Nature* 430, 75–78.

456 Soja C.M., 1994. Significance of Silurian stromatolite-sphinctozoan reefs. *Geology* 22,  
457 355–358.

458 Soja, C.M., Riding, R., 1993. Silurian microbial associations from the Alexander  
459 terrane, Alaska. *J. Paleont.* 67, 728–738.

460 Soja, C.M., Antoshkina, A.I., 1997. Coeval development of Silurian stromatolite reefs  
461 in Alaska and the Ural Mountains: Implications for paleogeography of the  
462 Alexander terrane. *Geology* 25, 539–542.

- 463 Soja, C.M., White, B., Antoshkina, A., Joyce, S., Mayhew, L., Flynn, B., Gleason, A.,  
464 2000. Development and decline of a Silurian stromatolite reef complex, Glacier  
465 Bay National Park, Alaska. *Palaios* 15, 273–292.
- 466 Textoris, D.A., Carozzi, A.V., 1966. Petrography of a Cayugan (Silurian) stromatolite  
467 mound and associated facies, Ohio. *Bull. Amer. Assoc. Petrol. Geol.* 50, 1375–  
468 1383.
- 469 Wan, Y., Zhang, T.S., Lan, G.Z., Yuan, J.X., 1997. The Silurian reef and its  
470 environmental evolution in the southeastern Sichuan Province and northern  
471 Guizhou Province. *Acta Sediment. Sin.* 15, 106–113 (in Chinese)
- 472 Wang, G., Li, Y., Kershaw, S., Deng, X.J., 2014. Global reef recovery after the  
473 end-Ordovician extinction: evidence from the late Aeronian  
474 coral-stromatoporoid reefs in South China. *GFF* 136, 286–289.
- 475 Wang, J.P., Deng, X.J., Wang, G., Li, Y., 2012. Types and biotic successions of the  
476 Ordovician reefs in China. *Chin. Sci. Bull.* 57, 1160–1168.
- 477 Watkins, R., 1979. Three Silurian bioherms of the Högklint Beds, Gotland.  
478 *Geologiska Foreningens i Stockholm Forhandlingar* 101, 33–48.
- 479 Wignall, P.B., Twitchett, R.J., 1999. Unusual intraclastic limestones in Lower Triassic  
480 carbonates and their bearing on the aftermath of the end-Permian mass  
481 extinction. *Sedimentology* 46, 303–316.
- 482 Yang, H., Chen, Z.Q., Wang, Y., Tong, J., Song, H., Chen, J., 2011. Composition and  
483 structure of microbialite ecosystems following the end-Permian mass extinction  
484 in South China. *Palaeogeogr. Palaeoclimatol. Palaeoecol.* 308, 111–128.

- 485 Zadoroshnaya, N.M., Nikitin, I.F., 1990. Kazakhstanskaya skladchataya oblast. In:  
486 Belenitskaya, G.A., Zadoroshnaya, N.M. (Eds.), Rifogennye i sulfatonosnye  
487 formatsii Fanerozoya SSSR (Phanerozoic Reefal and Sulfate bearing  
488 Formations of the USSR). Ministerstvo Geologii SSSR, Moscow, Nedra, pp.  
489 41–52 (in Russian)
- 490 Zhan, R.B., Jin, J.S., 2007. Ordovician–Early Silurian (Llandovery) Stratigraphy and  
491 Palaeontology of the Upper Yangtze Platform, South China. Science Press,  
492 Beijing, 169 pp..
- 493 Zhang, T.S., Lan, G.Z., Gao, W.D., Copper, P., 1994. Silurian reefs in northeast  
494 Sichuan, China. Science and Technology University Publishing House Science  
495 Press of Chengdu, Chengdu 115 pp. (in Chinese).
- 496 Ziegler, A.M., 1965. Silurian marine communities and their environmental  
497 significance. *Nature* 207, 270–272.

498

499 **Figure captions**

500 Fig. 1 Localities of four stromatolite deposits in the southern region and one  
501 metazoanal reef in the northern region sections in the Shihniulan Formation in north  
502 Guizhou. The southern region of these localities was Qianzhong Land closer to the  
503 location of stromatolite formation than the metazoan reefs. The greyish lines in the  
504 south and greyish dot line in the north are the coastlines of the beginning and end,  
505 respectively, of the Shihniulan Formation deposition (base palaeogeographic  
506 reconstruction map after Rong et al., 2012).

507

508 Fig. 2. Lithological logs of the four stromatolite-bearing sections in north Guizhou.

509

510 Fig. 3. Sedimentary features of the upper Shihniulan Member at Lianghekou section,

511 Xijiu, Xishui. (A) a cliff showing the horizons of stromatolite of (B) and (D) and

512 associated micritic limestone with birds-eye structures of (E). (B) stromatolitic unit in

513 dark grey silts and shales (lens cap = 8 cm for scale). (C) microfacies of the

514 stromatolite of B. (D) centimeter-scale stromatolite. E, micritic limestone with

515 birds-eye structures above the stromatolitic unit. (F) erosion surface as the

516 unconformable boundary between Shihniulan and overlying Hanchiatien formations.

517

518 Fig. 4. Successions of the Shihniulan Member, Shihniulan Formation at the Daijiagou

519 section, Tongzi. (A) mat-like stromatolites. (B) plan-view of columnar stromatolites;

520 the hammer is 28 cm long. (C) profile view of stromatolite columns. (D) small

521 loaf-shape stromatolite surrounded by greyish black siltstones and shales yielding

522 brachiopods *Lingulella* (a) and *Eospirifer* (b). (E) thin-bedded limestones with

523 cross-bedding above the stromatolitic units. (D) palaeokarst surface at the top of the

524 boundary between the Shihniulan and Hanchiatien formations.

525

526 Fig. 5. Microfacies of the stromatolites at the Daijiagou section. (A) calcimicrobial

527 mat-like stromatolite from the Bed 25. (B) columnar stromatolite from Bed 26.

528



529 Fig. 6. Lithological features of the stromatolites in the Shihniulan Member at the  
530 Baishanxi section, Tongzi. (A) thin-bedded nodular bioclastic limestone between the  
531 lower and upper stromatolitic units. (B–C) both upper (B) and lower (C) stromatolitic  
532 units are columnar. (D–E) pale laminations are common in both lower (D) and upper  
533 (E) stromatolitic units.

534

535 Fig.7. Lithological features of the stromatolites of the Shihniulan Member at Jianba  
536 section, Suiyang. (A) upper part of the Shihniulan Member showing the horizon of  
537 stromatolite-bearing unit; (B) columnar and dome-shaped stromatolites, white scale=8  
538 cm; (C–D) microfacies showing open spaces between stromatolitic laminae (C) and  
539 dolomitization of stromatolites locally (D).

540

541 Highlights:

- 542 1) Early Silurian biofacies differentiation on a carbonate ramp in the Upper Yangtze  
543 Platform were essentially controlled by depth of the sea.
- 544 2) Small-sized stromatolites formed in a regressional setting close to Qianzhong Land  
545 showing algal mat and column-shape.
- 546 3) Associated facies were typically formed in intertidal or/and lagoonal environments.
- 547 4) Tectonic uplift ended the deposition of limestones.

Figure1  
[Click here to download high resolution image](#)



Figure2  
[Click here to download high resolution image](#)

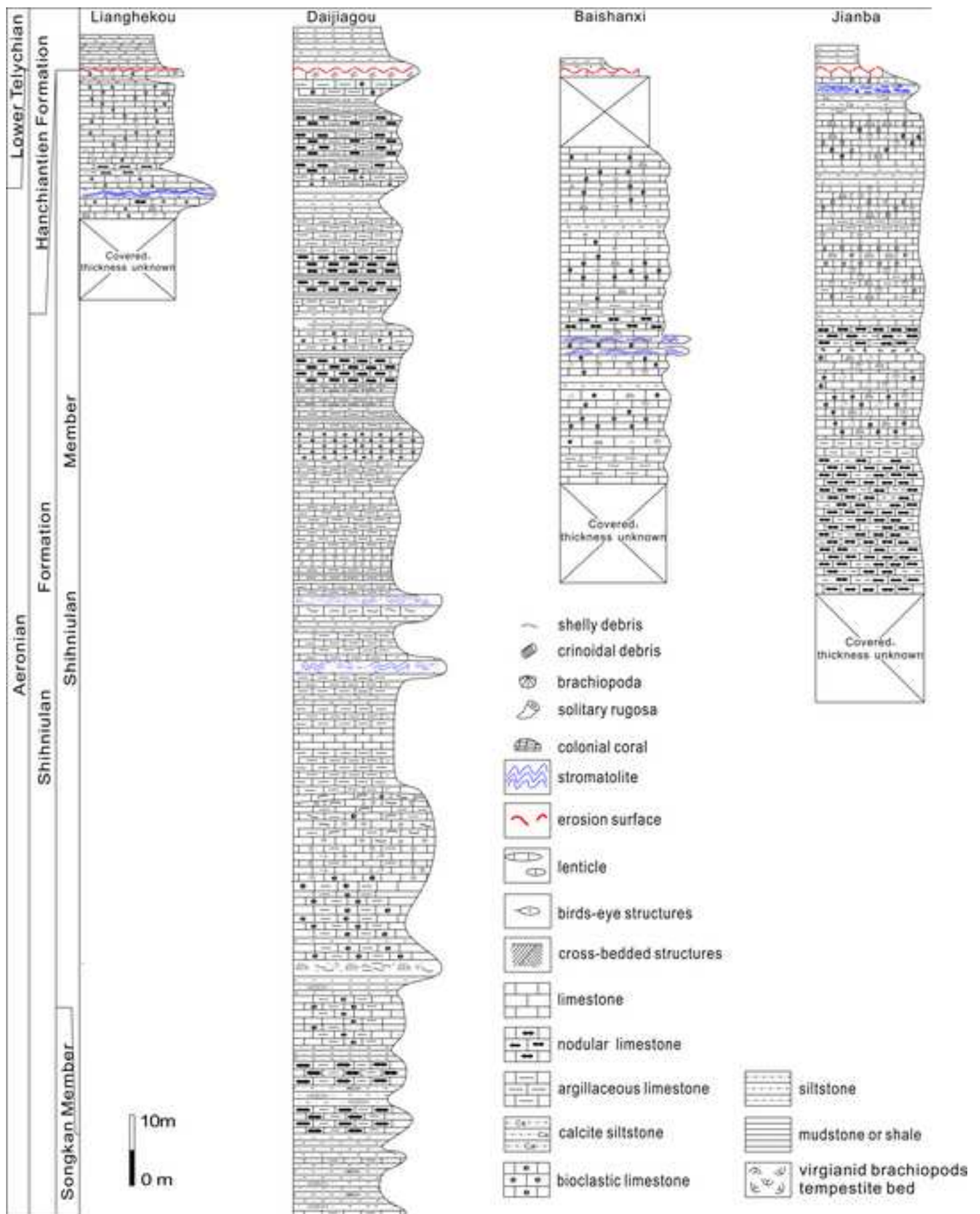




Figure3  
[Click here to download high resolution image](#)

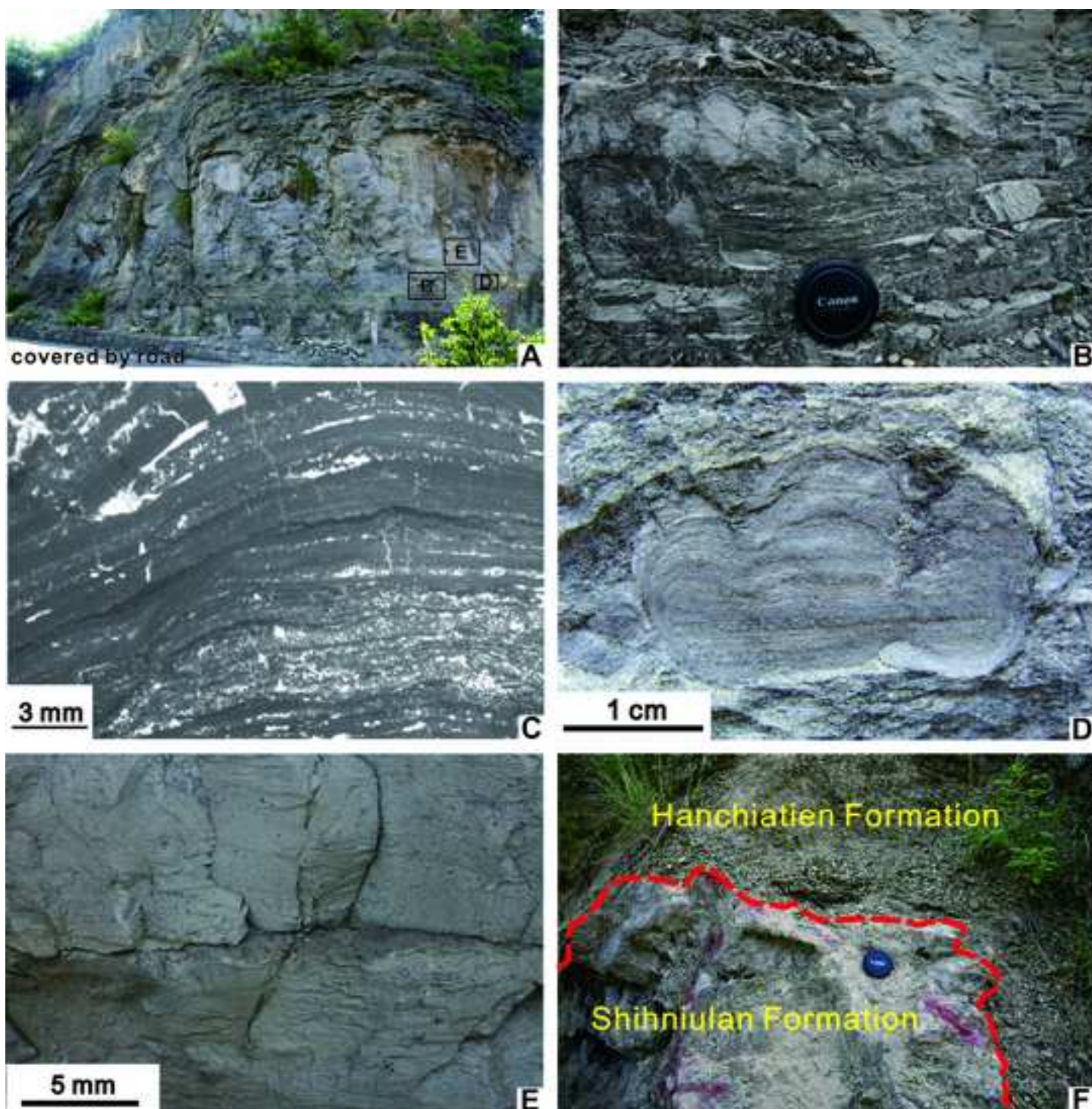
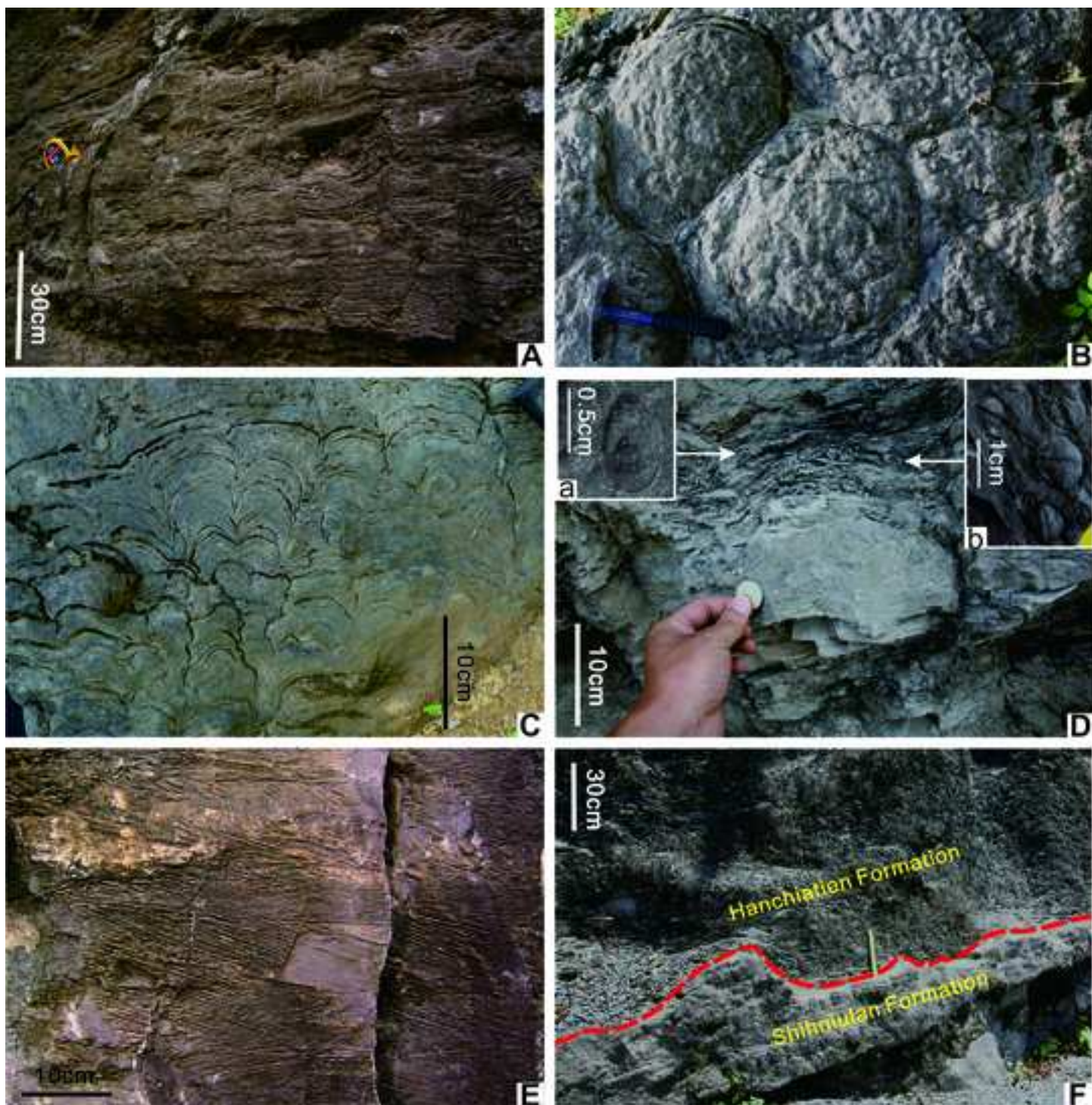




Figure4  
[Click here to download high resolution image](#)



**Figure5**  
[Click here to download high resolution image](#)

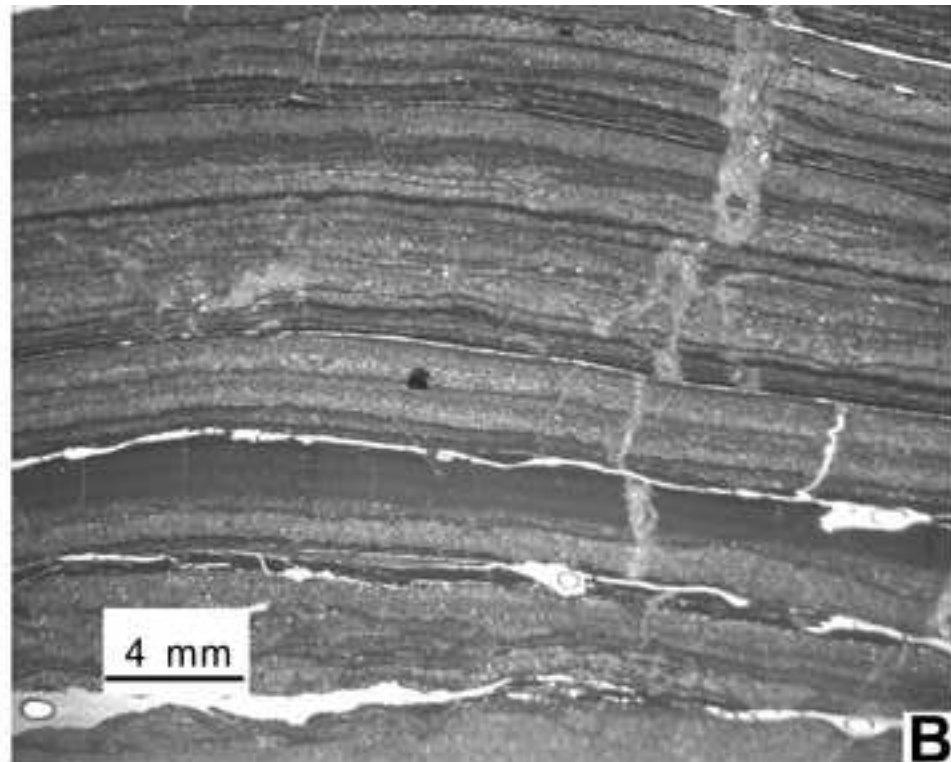
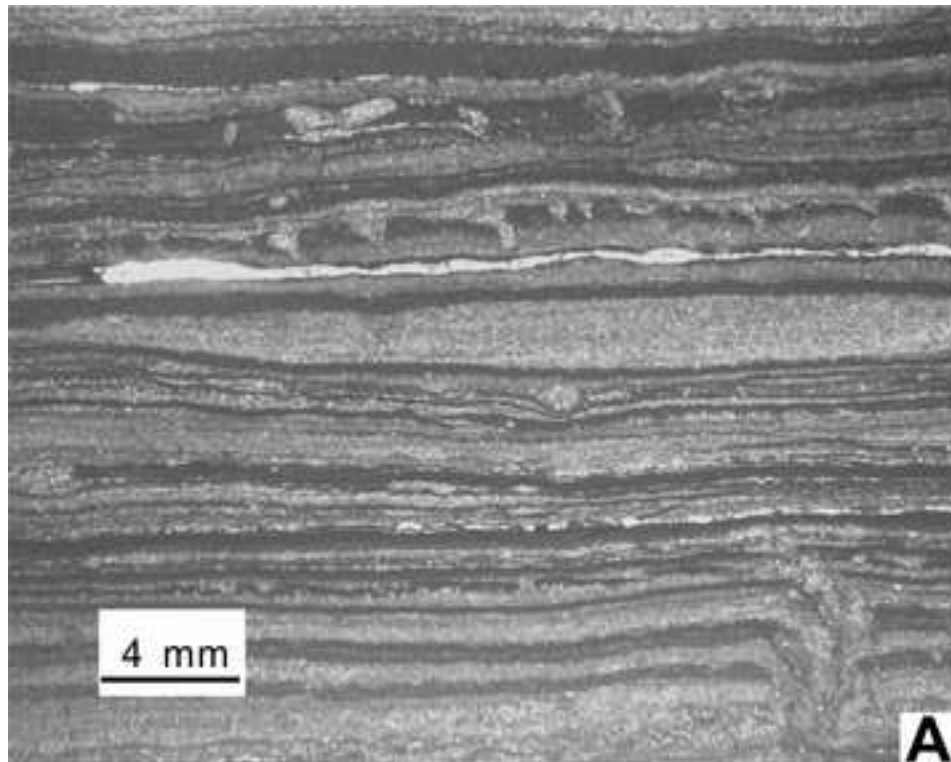




Figure 6  
[Click here to download high resolution image](#)

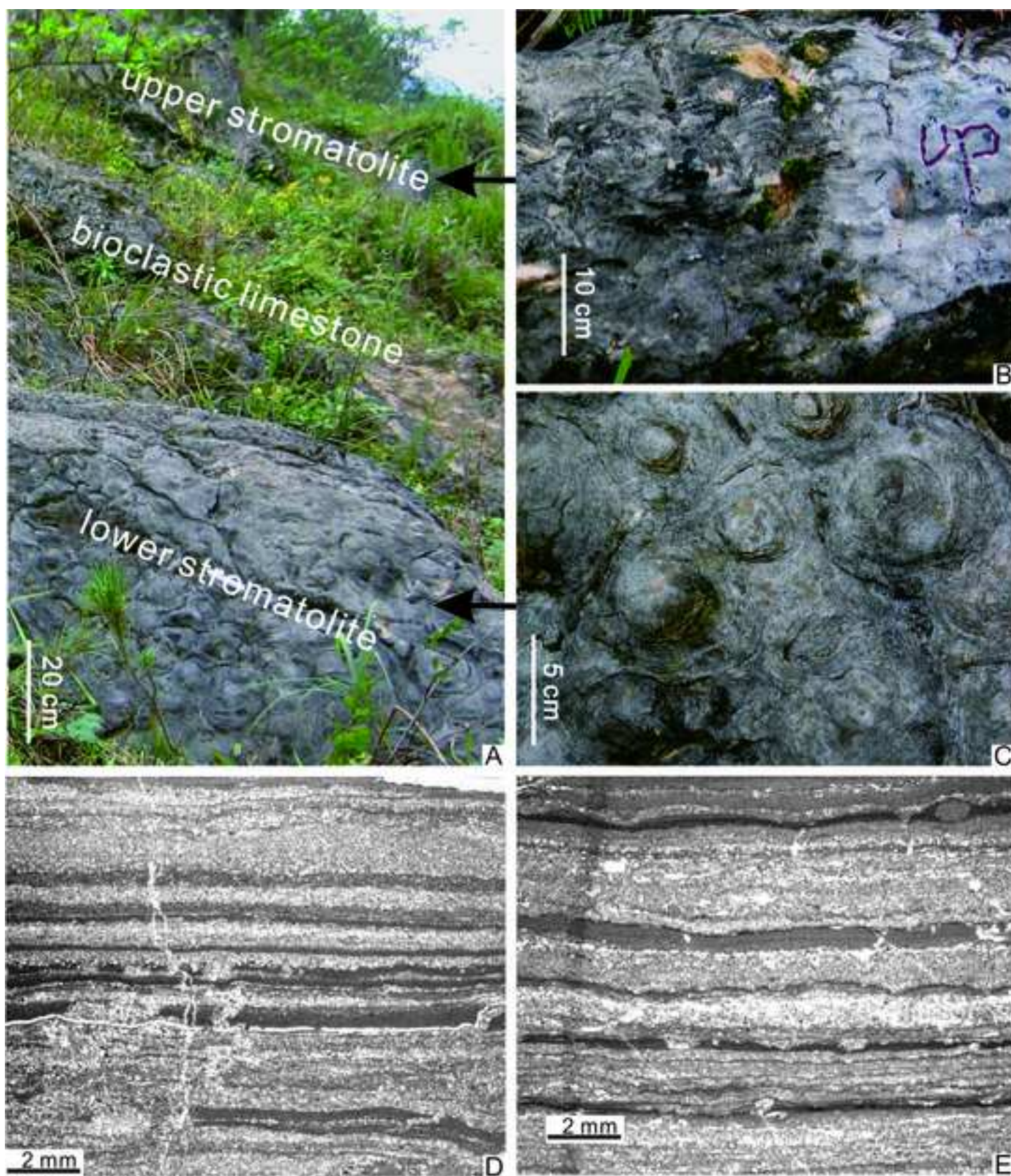




Figure7  
[Click here to download high resolution image](#)

